Fire-Resistance of Eccentrically Loaded Rectangular Concrete-Filled Steel Tubular Slender Columns Incorporating Interaction of Local and Global Buckling

Kamil, G. M., Liang, Q. Q. and Hadi, M. N. S. (2019). Fire-resistance of eccentrically loaded rectangular concrete-filled steel tubular slender columns incorporating interaction of local and global buckling. *International Journal of Structural Stability and Dynamics*, 19(8): 1950085.

FIRE-RESISTANCE OF ECCENTRICALLY LOADED RECTANGULAR CONCRETE-FILLED STEEL TUBULAR SLENDER COLUMNS INCORPORATING INTERACTION OF LOCAL AND GLOBAL BUCKLING

GHANIM MOHAMMED KAMIL and QING QUAN LIANG*

College of Engineering and Science, Victoria University, PO Box 14428, Melbourne, VIC 8001, Australia

**Qing.Liang@vu.edu.au*

MUHAMMAD N. S. HADI

School of Civil, Mining and Environmental Engineering, University of Wollongong, Wollongong, NSW 2522, Australia

A mathematical model using the fiber approach is presented in this paper for quantifying the strength and fire-resistance of eccentrically loaded slender concrete-filled steel tubular (CFST) columns with rectangular sections incorporating the interaction of local and global buckling. The model utilizes the thermal simulator to ascertain the temperature distribution in cross-sections, and the nonlinear global buckling analysis to predict the interaction responses of local and global buckling of loaded CFST slender columns to fire effects. The initial geometric imperfection, air gap between the concrete and steel tube, tensile concrete strength, deformations caused by preloads, and temperature-dependent material behavior are included in the formulation. The computational theory, modeling procedure and numerical solution algorithms are described. The computational model is verified by existing experimental and numerical results. The structural responses and fire-resistance of CFST columns of rectangular sections exposed to fire are investigated. The mathematical model proposed is demonstrated to

* Corresponding author. Tel.: 61 3 9919 4134.
E-mail address: Qing.Liang@vu.edu.au (Q. Q. Liang)

be an efficient computer simulator for the fire-performance of slender CFST columns loaded eccentrically.

Keywords: Concrete-filled steel tubes; Elevated temperatures; Fire-resistance; Interaction of local and global buckling; Nonlinear analysis.

1. Introduction

Thin-walled steel tubes are often used to construct slender square and rectangular concrete-filled steel tubular (CFST) columns in tall buildings to reduce the steel amounts to achieve economical designs.[1,2] However, eccentrically loaded slender CFST columns made of thin-walled rectangular sections under fire exposure may fail by the interaction of local and global buckling, which significantly reduces their ultimate strength and fire-resistance.[3,4] To provide realistic fire-resistance of such composite columns, inelastic modeling and design methods must consider the interaction of local and global buckling. However, because of the complexity of the interaction buckling problem, design methods specified in current design standards, such as Eurocode 4,[5] AISC-16[6] and ACI-318,[7] have not considered the interaction buckling effect on the fire behavior of slender rectangular CFST columns. In addition, the interaction of local and global buckling has rarely been included in theoretical models reported in the literature. This highlights the need for developing an efficient modeling technique including the interaction of local and global buckling, which is capable of accurately determining the fire resistance of slender CFST columns loaded eccentrically.

The fire response and resistance of CFST slender columns loaded axially or eccentrically have been studied experimentally by investigators.[8-15] Lie and Chabot[8] conducted standard fire tests

on six axially-loaded slender CFST square columns. The clear width-to-thickness (b/t_s) ratios of the tested columns ranged from 22 to 46. It was indicated that the failure of CFST square columns was caused by either the column global buckling or compression depending on the column slenderness. The report on the fire test results of eight slender CFST square columns fabricated by fire-resistant steel tubes loaded eccentrically was given by Sakumoto *et al.*[9] The report stated that the interaction of local and global buckling coupled with concrete crushing caused the failure of slender CFST columns with a b/t_s ratio of 31.3. Han *et al.*[10] performed experiments on two rectangular and one square eccentrically loaded slender CFST columns under fire exposure to ascertain their responses to fire effects. These CFST columns had the b/t_s ratios of 35.7 and 43.5. The fire test results signified that slender CFST box columns failed by the interaction of local and global buckling.

More recently, Espinos *et al.*[11,12] conducted fire tests on slender CFST box columns with and without reinforcing bars under large loading eccentricities. The rectangular columns had the b/t_s ratios of 23 and 33. Their results demonstrated that the failure mode of slender CFST rectangular columns with relatively large b/t_s ratios was the interaction of local and global buckling. The effect of the eccentricity of the applied load on the fire resistance was found to be detrimental. The nonlinear responses of eccentrically-loaded continuous CFST square columns constructed by plain concrete, bar-reinforced concrete and steel-fiber reinforced concrete exposed to fire were investigated experimentally by Ukanwa *et al.*[13] Due to the small b/t_s ratio of 31.3, all columns tested by Ukanwa *et al.* failed by the global buckling without local buckling. The bar-reinforced concrete improved the fire-resistance more than other types of concrete.

Fiber-based computational techniques have been formulated by several investigators to quantify the responses of loaded CFST columns to fire effects.[16-19] Lie and Irwin[17] proposed a numerical procedure for estimating the structural responses and fire resistance of CFST slender rectangular columns loaded axially with longitudinal steel bars exposed to fire. The numerical procedure considered the effects of concrete moisture content but ignored the concrete tensile strength and deformations induced by the preloads on the columns before being exposed to fire. Han[18] developed a computational model, which ascertained the fire resistance of square CFST beam-columns loaded eccentrically. The tensile strength and moisture content of concrete were not taken into consideration in the computational model, but it included the concrete confinement effect. An analysis technique was given by Chung *et al.*[19] that computed the fire resistance of square CFST slender columns subjected to eccentric loading. However, their technique did not account for the effects of the tensile strength and moisture content of concrete. It should be noted that the aforementioned theoretical models employing the fiber approach have not included the influences of the interaction of local and global buckling on the structural responses of CFST columns subjected to fire loading.

The commercial and specialized finite element (FE) programs have been utilized by a number of investigators to examine the fire performance of loaded slender CFST columns.[20-24] Ding and Wang[20] developed FE models using ANSYS to investigate the significance of the air gap and slip between the steel tube and concrete, concrete tensile strength, and initial imperfections on the responses of CFST columns to fire effects. It was concluded that including an air gap improved the accuracy of numerical predictions and the slip between the concrete core and steel tube had a minor influence on the predicted fire resistance. Hong and Varma[21] presented a sequentially coupled analytical procedure employing the FE program ABAQUS to examine the sensitivities of the fire behavior of CFST columns to the material constitutive models, concrete

tensile behavior, geometric imperfection, and local buckling. Schaumann *et al.*[22] utilized the FE software BoFIRE to compute the fire performance of circular and square CFST columns made of high-strength concrete. It was highlighted that local buckling effects have not been taken into account in most existing simulation techniques including BoFIRE, which leads to exaggerated predictions.

The above literature review has highlighted that the air gap between the concrete core and steel tube, concrete tensile strength, deformations caused by preloads, and interaction of nonlinear local and global buckling have not been included in existing fiber-based modeling method for CFST rectangular columns under fire exposure. To overcome these limitations, this paper presents an efficient mathematical model incorporating the aforementioned important features for simulating the fire resistance and responses of CFST slender columns of rectangular sections under uniaxial bending and axial compression. The formulation of the thermal and stress analyses, computer simulation procedure and solution algorithms for slender CFST columns under fire exposure are provided. Comparisons of calculations with existing experimental and numerical results are conducted to validate the proposed model. A parametric study is performed to ascertain the significance of various factors on the fire resistance and structural responses of CFST columns under fire exposure.

2. Thermal Analysis

2.1. *The method of fiber element analysis*

The thermal simulator utilizes the computationally efficient and accurate method of fiber elements to discretize the cross-sections of rectangular CFST columns as suggested by

Liang.[25,26] The method of fiber elements is computationally more efficient than the traditional finite element method as the fiber method does not require the discretization of the column along its length.[27] Figure 1 illustrates the typical fiber mesh for the cross-section, which is discretized into square elements of fibers. The size of steel fiber elements is equal to half of that of concrete fiber elements. Each fiber is given to either concrete or steel properties at elevated temperatures. In addition, each fiber is assigned to a temperature in accordance with the calculated temperature distribution in the thermal analysis. The longitudinal stresses are computed from axial strains by means of applying the stress-strain constitutive laws of steel as well as concrete, which are temperature-dependent. The axial force (P) as well as bending moment (M_x) in the cross-section are calculated by stress integrations.[25]

The assumptions underlying the formulation of the fiber model are: (1) the rectangular CFST slender column is exposed to uniform temperatures along its length; (2) a perfect bond between the steel tube and concrete infill exists; (3) the plane section remains plane after deformation; (4) the local buckling of thin-walled steel tubes is considered; (5) an air gap at the steel-concrete interface is incorporated; (6) the tensile behavior of concrete is taken into account; (7) the shrinkage and creep of concrete are ignored.

2.2. *Temperature calculations*

It is assumed that the temperature distributions around the four sides of a CFST column of rectangular section exposed to fire and along its length are uniform. The temperatures on the surfaces of the CFST column under fire exposure are calculated by the standard temperature-time equation provided in Eurocode 1.[28] The method of finite difference is used to numerically solve the heat equation in 2D to ascertain the nodal temperatures at elements within the column

cross-section. The element temperature at its centroid is taken as its average nodal temperatures. The thermal analysis requires the input of three main material thermal properties, which include density, specific heat and thermal conductivity. The thermal properties of steel given in Eurocode 3[29] and those of concrete presented by Lie and Irwin[17] are adopted in the present study. An air gap between the concrete and steel tube with a contact resistance of 100 W/m^{2}K is considered in the thermal model as suggested by Ding and Wang.[20] The value of the exposure surfaces emissivity is specified as 0.7. The concrete moisture content is assumed to be 3% as suggested by Eurocode 2.[30] The detailed thermal analysis procedure can be found in the paper by Kamil *et al.*[31]

3. Nonlinear Stress Analysis of Cross-sections

3.1. *Strain calculations*

The strain distribution through the depth of the column cross-section under combined uniaxial bending and axial compression is assumed to be linear as schematically illustrated in Fig. 1. For CFST columns under fire exposure, the longitudinal strain consists of the component induced by the applied load and bending moment, and the component caused by the fire effect. The strains are calculated by the following equations:

$$y_{n,i} = \frac{D}{2} - d_n \tag{1}$$

$$d_{e,i} = | y_i - y_{n,i} | \tag{2}$$

$$\varepsilon_i = \begin{cases} \phi d_{e,i} - \varepsilon_T & \text{for } y_i \geq y_{n,i} \\ -\phi d_{e,i} - \varepsilon_T & \text{for } y_i < y_{n,i} \end{cases} \tag{3}$$

where D denotes the section depth, d_n represents the neutral axis depth of the cross-section, y_i stands for the coordinate of the fiber i, ε_i defines the strain of the element i, and ε_T represents the thermal strain corresponding to steel or concrete element.

3.2. *Temperature-dependent stress-strain model for steel*

The present mathematical model employs the temperature-dependent stress-strain model for structural steels recommended by Eurocode 3.[29] The typical uniaxial stress-strain curves for steel as a function of temperatures in accordance with Eurocode 3 have been plotted in Fig. 2, which are expressed by

$$\sigma_{s,T} = \begin{cases} E_T \varepsilon_s & \text{for } \varepsilon_s \le \varepsilon_{p,T} \\ \left(f_{p,T} - h_3\right) + \dfrac{h_2}{h_1}\sqrt{h_1^2 - \left(\varepsilon_{y,T} - \varepsilon_s\right)^2} & \text{for } \varepsilon_{p,T} < \varepsilon_s \le \varepsilon_{y,T} \\ f_{y,T} & \text{for } \varepsilon_{y,T} < \varepsilon_s \le \varepsilon_{t,T} \\ f_{y,T}\left[1 - \left(\varepsilon_s - \varepsilon_{t,T}\right)/\left(\varepsilon_{u,T} - \varepsilon_{t,T}\right)\right] & \text{for } \varepsilon_{t,T} < \varepsilon_s \le \varepsilon_{u,T} \\ 0 & \text{for } \varepsilon_s > \varepsilon_{uT} \end{cases} \tag{4}$$

in which

$$h_1^2 = (\varepsilon_{y,T} - \varepsilon_{p,T})(\varepsilon_{y,T} - \varepsilon_{p,T} + h_3 / E_T) \tag{5}$$

$$h_2^2 = E_T(\varepsilon_{y,T} - \varepsilon_{p,T})h_3 + h_3^2 \tag{6}$$

$$h_3 = \frac{(f_{y,T} - f_{p,T})^2}{E_T\ (\varepsilon_{y,T} - \varepsilon_{p,T}) - 2\ (f_{y,T} - f_{p,T})} \tag{7}$$

where E_T is the elastic modulus of steel, $f_{p,T}$ denotes the proportional stress limit, $f_{y,T}$ stands for the yield stress, $\varepsilon_{p,T}$ stands for the strain at proportional limit, $\varepsilon_{y,T}$ represents the yield strain, and $\varepsilon_{u,T}$ is the ultimate strain of steel at elevated temperatures.

Elevated temperatures remarkably reduce the strength and stiffness of steel material. Eurocode 3[29] provides reduction factors that are used to reduce the material properties of steel at higher temperatures. The reduction factor applied to the proportional limit is denoted as $R_{p,T}$, to the steel yield strength is represented by $R_{y,T}$, and to the steel modulus of elasticity at elevated temperatures is $R_{E,T}$. The values of these reduction factors are given in Eurocode 3 and the paper by Kamil *et al.*[31] and therefore are not given here. When the temperature is below 400ºC, the strain hardening is considered in the present computational model in accordance with Eurocode 3.[29]

3.3. *Temperature-dependent stress-strain model for concrete*

The temperature-dependent stress-strain curve for filled concrete in CFST columns is depicted in Fig. 3. The present fiber-based mathematical model utilizes the stress-strain relations of concrete at elevated temperatures described in Eurocode 2.[30] For concrete in compression, the longitudinal stresses of concrete are calculated from axial strains by

$$\sigma_{c,T}=\begin{cases}\dfrac{3\varepsilon_c f'_{c,T}}{\varepsilon'_{c,T}\left[2+\left(\varepsilon_c/\varepsilon'_{c,T}\right)^3\right]} & \text{for } \varepsilon_c \le \varepsilon'_{c,T}\\ f'_{c,T}\left[\dfrac{\varepsilon_{cu,T}-\varepsilon_c}{\varepsilon_{cu,T}-\varepsilon'_{c,T}}\right] & \text{for } \varepsilon_c > \varepsilon'_{c,T}\end{cases} \tag{8}$$

where $f_{c,T}^{'}$ is the compressive concrete strength of concrete, $\varepsilon_{c,T}^{'}$ is the strain at $f_{c,T}^{'}$, and $\varepsilon_{cu,T}$ denotes the ultimate strain of concrete at elevated temperatures. The values of $\varepsilon_{c,T}^{'}$ and $\varepsilon_{cu,T}$ of concrete made of siliceous aggregates at elevated temperatures are given in Eurocode 2.[30]

It should be noted that the stress-strain model for concrete at elevated temperatures given in Eurocode 2[30] does not consider the confinement effect as the steel tube provides little confinement to the concrete in rectangular and square CFST columns and the confinement is limited to the column corners.[1-4] In addition, the high temperature and local buckling significantly reduce the strength and stiffness of the rectangular steel tube, which provides no confinement to the concrete core so that it is neglected in the present study. However, in the post-fire nonlinear analysis of CFST columns, the confinement model for concrete has been used by Yang et al.[32]

The tensile strength of concrete has a noticeable influence on the fire behavior of CFST columns and is therefore considered in the present computational model. The stress-strain response of concrete in tension is described by two-linear curves as shown in Fig. 3. At ambient temperatures, the concrete tensile strength is taken as 10% of its compressive strength. At elevated temperatures, the reduction factor given in Eurocde 3[29] is applied to the tensile concrete strength. The ultimate tensile strain of concrete at which the tensile stress is zero is specified as 10 times the cracking strain.

3.4. *Modeling local and post-local buckling*

The reduction in the fire resistance of CFST slender columns due to local buckling is significant as reported by Kamil *et al.*[31] Thus, the present mathematical modeling method incorporates the

influence of local and post-local buckling on the structural performance of slender CFST columns with rectangular sections under fire. Kamil *et al.*[33] developed equations that predict the critical local buckling stresses of steel plates subjected to non-uniform in-plane stresses in CFST columns exposed to fire. These equations, which considered the local geometric imperfection in addition to residual stresses, are used in the proposed numerical scheme to ascertain the initial local buckling stresses of CFST slender columns under fire exposure.

The post-local buckling strength of thin steel plates can be computed by the effect width method as discussed by Liang[26] and Liang *et al.*[34] The typical effective widths of steel tube in a CFST columns of rectangular section under uniaxial bending are illustrated in Fig. 4. The effective width expressions for steel plates subjected to stress gradients in rectangular CFST columns under fire exposure constructed by Kamil *et al.*[33] are implemented in the proposed mathematical model, which are written as

$$\frac{b_{e1}}{b}=\frac{1}{2}(q_1\lambda_{c,T}^{q})\frac{0.8418\lambda_{c,T}^{0.02368}\left(\frac{R_{p,T}}{R_{y,T}}\right)^{-0.3028}+1.154\left(\frac{R_{p,T}}{R_{y,T}}\right)}{2.055+\lambda_{c,T}^{1.68}} \qquad (\alpha_s>0) \tag{9}$$

$$\frac{b_{e1}}{b}=\frac{1}{3}(q_1\lambda_{c,T}^{q})\frac{0.8418\lambda_{c,T}^{0.02368}\left(\frac{R_{p,T}}{R_{y,T}}\right)^{-0.3028}+1.154\left(\frac{R_{p,T}}{R_{y,T}}\right)}{2.055+\lambda_{c,T}^{1.68}} \qquad (\alpha_s=0) \tag{10}$$

$$\frac{b_{e2}}{b}=(2-\alpha_s)\frac{b_{e1}}{b} \tag{11}$$

where b_{e1} and b_{e2} denote the effective widths depicted in Fig. 4, b is the clear width of the steel plate, α_s represents the stress gradient coefficient, which is defined by the ratio of the minimum to the maximum in-plane stresses on the plate, q and q_1 are expressed by

$$q = 0.04007\alpha_s^2 - 0.05275\alpha_s + 0.03355 \tag{12}$$

$$q_1 = 0.1007\alpha_s^2 - 0.7027\alpha_s + 1.65 \tag{13}$$

The relative slenderness ratio $\lambda_{c,T}$ of the steel plate at elevated temperature is described by

$$\lambda_{c,T} = \sqrt{\frac{12(1-\nu^2)(b/t_s)^2(R_{y,T}f_y)}{k\pi^2(R_{E,T}E)}} \tag{14}$$

in which f_y represents the steel yield strength at room temperature, ν denotes the Poisson's ratio of steel, E stands for the Young's modulus of steel material at room temperature, and the elastic local buckling coefficient k of a steel plate with clamped boundary conditions is given as 9.95 by Kamil *et al.*[33]

In the regime of post-local buckling, a thin steel plate subjected to increasing load can gradually redistribute the in-plane stresses from the heavily buckled region to the edge strips.[26] The ineffective widths of the steel flange and webs as depicted in Fig. 4 increase as the loading increases until their ultimate strengths are attained. The stresses of steel fibers within the ineffective widths are given to zero in accordance with the effective width concept. The unique numerical modeling scheme proposed by Liang[25] has been used in the proposed computational method to model the gradual post-local buckling of steel tubes of CFST columns exposed to fire.

4. Nonlinear Global Buckling Analysis of Slender Columns

4.1. *Formulation of computational theory*

Eccentrically loaded pin-ended slender CFST columns under fire exposure are considered in the present study. It is assumed that the slender column exposed to fire is under single curvature bending about its principal axis. The part-sine function is used to represent the lateral displacement of the slender column as suggested by Liang[35], and is written by

$$u = u_m \sin\left(\frac{\pi z}{L}\right) \tag{15}$$

where u_m is the lateral deflection occurs at the column mid-length, and L is its effective length.

The curvature induced at the column mid-length can be obtained from the displacement shape function as

$$\phi_m = u_m \left(\frac{\pi}{L}\right)^2 \tag{16}$$

The CFST columns used in composite buildings are subjected to vertical loads from upper floors. The eccentric loading applied to the CFST column before being exposed to fire causes initial lateral displacement and stresses within the column. This constant eccentric load is considered as a preload on the column as discussed by Patel *et al.*[36] The computational procedure of load-deflection is used to quantify the lateral deflection due to the preload, which is incorporated in the global buckling simulation of slender CFST columns exposed to fire as an additional initial geometric imperfection (u_{po}). The mathematical formulation also accounts

for the initial geometric imperfection (u_o) and lateral displacement (u_m) at the column mid-height. The external bending moment acting at the column mid-height becomes

$$M_{ext} = P(u_{po} + u_o + e + u_m) \tag{17}$$

where *e* represents the loading eccentricity at the ends of the column and the initial geometric imperfection u_o at the column mid-height can be taken as *L*/1000.

The present mathematical modeling technique employs the method of displacement control to compute the complete load-lateral displacement responses of CFST slender columns to fire effects. In this method, the lateral displacement at the column mid-height is incrementally increased. The internal axial force corresponding to this lateral displacement is computed. The internal axial force satisfying the moment equilibrium at the column mid-height is treated as the external applied axial load at the column ends with an eccentricity (*e*). The process of calculations is repeated until the complete axial load-displacement curve is determined. The function of residual moment generated in the computation is constructed as

$$r_M = M_x - P(u_{po} + u_o + e + u_m) \tag{18}$$

In the numerical computation, if $|r_M| < \varepsilon_k = 10^{-4}$, the moment equilibrium condition is satisfied.

The fire resistance of an eccentrically loaded CFST slender column under fire exposure is determined by gradually increasing the fire temperature and calculating the axial load-lateral displacement responses of the column to the fire effects. The column ultimate strength decreases with an increase in the time of fire exposure. The fire resistance of the CFST column

is obtained as the fire exposure time that reaches the failure point of the column. The computer simulation procedure for quantifying the fire-resistance of a slender rectangular CFST column loaded eccentrically is generally incremental and iterative and is described as follows:

(1) Input data.

(2) Mesh the CFST cross-section into fiber elements and compute their areas and coordinates.

(3) Compute the lateral displacement of the slender CFST column under constant preload.

(4) Initialize the fire exposure time as $t = \Delta t$.

(5) Calculate temperatures on column surfaces and at fiber elements within its cross-section.

(6) The lateral deflection at the column mid-length is specified as $u_m = \Delta u_m$.

(7) Compute the mid-height curvature ϕ_m of the slender column.

(8) Adjust the neutral axis depth (d_n) by employing solution algorithms implementing Müller's method.[37]

(9) Calculate element stresses from strains by temperature-dependent stress-strain models for concrete as well as steel.

(10) Simulate the gradual local and post-local buckling of steel tube with thin-walled section.

(11) Compute the sectional axial force P and moment M_x.

(12) Determine the residual moment function r_M.

(13) Repeat Steps 8 to 12 until $|r_M| < \varepsilon_k = 10^{-4}$.

(14) Increase the lateral deflection at the column mid-height by $u_m = u_m + \Delta u_m$.

(15) Repeat Steps 7 to 14 until $P < 0.5P_u$ or the deflection is beyond the specified limit.

(16) Increase the fire exposure time by $t = t + \Delta t$.

(17) Repeat Steps 5 to 16 until the fire resistance of the CFST column is obtained.

4.2. *Algorithms for solving nonlinear dynamic functions*

As described in the proceeding section, the neutral axis depth (d_n) of the cross-section needs to be adjusted iteratively to achieve the equilibrium condition at the column mid-height. The residual moment function generated in the incremental-iterative analysis process is changing at each iteration so it is dynamic. The highly nonlinear dynamic function is not derivative with respect to the design variables. Computational algorithms implementing Müller's method[37] have been developed to ascertain the true depth of the neutral axis in the column cross-section.[3,4] The numerical technique requires three initial neutral axis depths $d_{n,1}$, $d_{n,2}$ and $d_{n,3}$ to start the computation process. The new neutral axis depth $d_{n,4}$ is determined by

$$d_{n,4} = d_{n,3} + \frac{-2c_m}{b_m \pm \sqrt{b_m^2 - 4a_m c_m}} \tag{19}$$

$$a_m = \frac{(d_{n,2} - d_{n,3})(r_{M,1} - r_{M,3}) - (d_{n,1} - d_{n,3})(r_{M,2} - r_{M,3})}{(d_{n,1} - d_{n,2})(d_{n,1} - d_{n,3})(d_{n,2} - d_{n,3})} \tag{20}$$

$$b_m = \frac{(d_{n,2} - d_{n,3})^2(r_{M,2} - r_{M,3}) - (d_{n,2} - d_{n,3})^2(r_{M,1} - r_{M,3})}{(d_{n,1} - d_{n,2})(d_{n,1} - d_{n,3})(d_{n,2} - d_{n,3})} \tag{21}$$

$$c_m = r_{M,3} \tag{22}$$

In Eq. (19), the signs of b_m and the square root term in the denominator are taken as the same. The computations using above equations are undertaken to iteratively adjust the neutral axis depth until the equilibrium condition is achieved.[3,4]

5. Verification of the Fiber-Based Mathematical Model

The mathematical model has been developed for eccentrically loaded slender rectangular and square CFST columns constructed by normal strength plain concrete and normal strength thin-walled steel tubes. Therefore, existing numerical and test data on the fire-resistance of eccentrically loaded CFST columns constructed by normal strength plain concrete and normal strength thin-walled steel tubes were employed to verify the model. Standard fire tests on slender CFST columns under eccentric loading were undertaken by Han *et al.*[10], Espinos *et al.*[12], Kordina and Klingsch[38] while Ding and Wang[20] carried out finite element analyses on the structural responses of eccentrically loaded CFST square columns to fire effects. The geometry as well as steel and concrete properties of these columns are given in Table 1. The computer simulation technique developed was used to determine the fire-resistance of the columns whose details are provided in Table 1.

It would appear from Fig. 5 that the fire-resistance in time predicted by the fiber-based computing technique are generally in good correlations with those determined from the standard fire tests and finite element analyses. However, there is a discrepancy between the predictions by the present mathematical model and experimental and finite element results. The causes for this discrepancy are: (a) measurements on the steel and concrete thermal properties of the tested columns were not undertaken and might be different from those implemented in the present computational model; (b) the actual concrete moisture content in the tested columns was unknown and might not be equal to the specified value in the present model; (c) only part of the column length was heated in the standard fire tests.

6. Parametric Study

The developed computer simulation technique was used to ascertain the significance of various parameters on the structural responses as well as fire resistance of eccentrically loaded CFST columns under fire exposure. In parametric study, the Young's modulus of steel at room temperature was 210 GPa. All CFST columns under investigation were assumed to have an initial out-of-plane displacement of $L/1000$ at the column mid-length.

6.1. *Influences of local buckling of steel tubes*

Local buckling may occur in thin-walled CFST short columns, which do not undergo global buckling so that there is no interaction between local and global buckling in CFST short columns. However, when the length of the thin-walled CFST column is increased from short to slender, local and global buckling may take place simultaneously so that there is an interaction between local and global buckling. Local buckling reduces the stiffness and strength of the CFST slender column, which may cause the global buckling of the column. The significance of local buckling on the structural responses and fire-resistance of CFST columns loaded eccentrically was examined by using the computer program developed. A square CFST column with the dimensions of 500×500×5 mm constructed by a steel tube having a yield stress of 300 MPa and 40 MPa concrete was employed. The column, which had a member slenderness ratio (L/r) of 25 and a loading eccentricity ratio (e/D) of 0.05, was analyzed by incorporating local buckling as well as ignoring it, respectively. The computed load-lateral displacement responses of the column at 20 min fire exposure are shown in Fig. 6. It is found that the column ultimate strength at 20 min fire-exposure is reduced by 7% due to local buckling. The influence of local buckling on the column strength-fire exposure time curve is illustrated in Fig. 7. It would appear that the effect of local buckling on the column ultimate load is found to be the most prominent at ambient temperature, which leads to 9% reduction in the column strength. However, its

influence decreases as the time of fire exposure increases. After 40 min fire exposure, local buckling has an insignificant influence on the fire-resistance and can be ignored. Based on the effective width formulas, local buckling would reduce the axial capacity of the hollow steel tube by up to 60%.[33] When compared with the capacity of the CFST column, this percentage reduction decreases. However, if normal-strength concrete and high-strength steel tube are used to construct the CFST column that is not too slender, the reduction in column strength due to local buckling is significant and should be taken into consideration in numerical simulations.

6.2. *Influences of column slenderness*

Square columns of 600×600 mm with a B/t_s ratio of 60 and various member slenderness ratios were analyzed to ascertain the effects of the *L*/*r* ratio on their responses to fire loading. The columns had an *e*/*D* ratio of 0.1, steel yield strength of 350 MPa and concrete strength of 45 MPa. The column slenderness ratios were computed as 22, 32, 42 and 50 by varying the column length. The computational axial load-lateral displacement curves for these columns at 40 min fire-exposure have been plotted in Fig. 8. It is clearly shown that increasing the *L*/*r* ratio remarkably reduces the column ultimate axial load in addition to its initial stiffness. When changing *L/r* ratio from 22 into 32, 42 and 50, the ultimate strength of the column decreases by 8%, 20% and 31%, respectively, and the lateral deflection at the ultimate load increases from 14 mm to 28.5 mm, 46.5 mm and 63 mm, respectively. Figure 9 gives the column strength-fire exposure time curves for CFST columns as a function of member slenderness ratios. It is apparently demonstrated that the column strength decreases markedly as a result of increasing the fire exposure time regardless of the *L*/*r* ratio. At 20 min fire-exposure, changing the *L*/*r* ratio from 22 to 32, 42 and 50 results in a reduction in the column strength by 8%, 21% and 39%, respectively. However, at 60 minutes of heating, changing the *L*/*r* ratio from 22 to 32, 42 and

50 results in a strength reduction by 10%, 24% and 38%, respectively. It is noted that the column with the *L*/*r* ratio of 50 has the lowest strength at the fire exposure time of about 20 min. This is due to the interaction of local and global bucking in slender CFST column and the load is transferred from the buckled steel tube to the concrete core.

6.3. *Influences of loading eccentricity ratio*

Nonlinear fire response analyses on a slender square CFST column, which had a cross-section of 400×400 mm, B/t_s ratio of 80 and *L/r* ratio of 32, were performed to ascertain the significance of *e*/*D* ratios on their fire behavior. The compressive strength of the filled concrete was 40 MPa while the steel yield stress was 300 MPa. The column was subjected to applied loads with the eccentricity ratios of 0.05, 0.1, 0.15 and 0.2. The structural responses of the column having various *e*/*D* ratios at 40 min fire-exposure are presented in Fig. 10. The column ultimate load and initial stiffness are reduced greatly by increasing the end eccentricity of applied loads. The sensitivity of the column strength-fire exposure time curves to the *e*/*D* ratio is illustrated in Fig. 11. When the *e*/*D* ratio is changed from 0.05 into 0.1, 0.15 and 0.2, the column strength at ambient temperatures decreases by 11%, 20% and 28%, respectively, but at 20 min fire exposure, it decreases by 17%, 30% and 49%, respectively.

6.4. *Influences of compressive concrete strength*

The significance of the compressive strength of filled concrete on the structural responses of CFST rectangular columns in fire was investigated by means of employing the computer program developed. The CFST columns under investigations had the following properties: cross-section of 400×450 mm having a thickness of 10 mm, yield strength of 350 MPa, *L*/*r* ratio

of 35, and *e*/*D* ratio of 0.1. The compressive strengths of the filled concrete in these columns ranged from 25 MPa to 55 MPa. Figure 12 gives the axial load-lateral deflection relationships of CFST columns with different concrete strengths at 40 min fire exposure. It is distinctly indicated that increasing the concrete strength leads to a remarkable improvement in the ultimate load as well as initial stiffness of the CFST columns. It is observed from the column strength-fire time curves depicted in Fig. 13 that the use of higher strength concrete appreciably improves the column strength regardless of the time of fire exposure. In addition, the effect of concrete strength on the column strength increases as the time of fire exposure increases. When changing the concrete strength from 25 to 35MPa, 45 MPa and 55 MPa, at ambient temperature, the percentage increase in the column axial load is 16%, 32% and 47%, respectively; however, at 40 min fire-exposure, it becomes 40%, 80% and 120%, respectively.

6.5. Influences of steel yield strength

The fire behavior of square CFST columns fabricated by steel tubes having yield strengths ranging from 250 MPa to 450 MPa was studied. The details of the columns under consideration were: section of 500×500 mm, B/t_s=100, $f_c^{'}=35$ MPa, L/r =30, and e/D=0.1. Figure 14 presents the significance of the steel yield stress on the column strength-fire exposure time curves. It is confirmed that the influence of steel yield stress on the column strength is the most prominent at room temperature. Its impact decreases considerably as a result of increasing the time of fire exposure. After 20 min fire exposure, however, the ultimate axial strength of the CFST columns is not affected by the steel yield stress.

6.6. Influences of width-to-thickness ratio

The computational technique proposed was used to investigate the effect of B/t_s ratio on the performance of CFST columns in a fire environment. The CFST columns having a square section of 350×350 mm, concrete strength of 55 MPa, steel yield strength of 450 MPa, *e*/*D* ratio of 0.1, *L*/*r* ratio of 40, and B/t_s ratios of 40, 60, 80 and 100 were analyzed under fire loading. The significance of the B/t_s ratio on the fire-exposure time-column strength curves is demonstrated in Fig. 15. The influence of the B/t_s ratio on the column ultimate load is most pronounced at room temperature but increasing the fire exposure time decreases its impact. After 20 min fire exposure, its effect becomes insignificant. At room temperature, changing the B/t_s ratio from 40 to 60, 80 and 100 decreases the column strength by 16%, 25% and 29%, respectively. In contrast, at 40 min fire exposure, it increases the column strength by only 4%, 7% and 6%, respectively. The cause for this is that the elevated temperature sustainably reduces the strength and stiffness of steel material, which minimizes the effect of the B/t_s ratio. In addition, the load transmission from the steel tube to the concrete takes place. At elevated temperatures, the column with a smaller B/t_s ratio has a smaller concrete area so that it has a lower strength.

6.7. Influences of preloads

The CFST column with a square section of 400×400 mm and a B/t_s ratio of 80 subjected to preloads and fire loading was analyzed. The yield strength of steel tube was 350 MPa and the concrete had a compressive strength of 45 MPa. The column slenderness ratio was 60 and the load was applied with an *e*/*D* ratio of 0.1. The preload ratios (β) of 0.0, 0.4 and 0.6 were selected in numerical analyses. Figure 16 presents the column axial strengths which are dependent on the fire exposure time and preload ratio. It is indicated that the column strength

decreases with an increase in the preload regardless of the fire exposure time. At ambient temperature, when changing the preload ratio from 0.0 to 0.4 and 0.6, the column strength is shown to decrease by 4% and 6%, respectively. It would appear from Fig. 16 that the most pronounced strength reduction occurs at 20 min fire exposure. At this time, the column strength was reduced by 12% and 21%, respectively, by increasing the preload ratio from 0.0 to 0.4 and 0.6.

7. Conclusions

This paper has presented a mathematical model utilizing the fiber approach for the determination of the structural responses and fire resistance of eccentrically loaded slender CFST columns with rectangular sections under fire exposure. The computer model has incorporated various important features associated with slender thin-walled rectangular CFST columns exposed to fire, including air gap between the concrete and steel tube, concrete tensile strength, deformations induced by preloads and the interaction of nonlinear local and global buckling, which have not been considered in other fiber-based numerical models. The computational model developed has been verified by independently established experimental and numerical results.

The results obtained from the parametric study have confirmed that the local buckling effect on the strength of CFST columns is the most prominent at room temperature and its effect decreases as the time of fire exposure increases. The column strength and stiffness are remarkably reduced by increasing either the columns slenderness or the loading eccentricity. The use of higher strength concrete significantly improves the column strength, stiffness, and fire-resistance and its effect increases when the time of fire exposure increases. Increasing the

steel yield strength notably improves the column strength but after 20 min fire exposure its effect diminishes. The tube width-to-thickness ratio has the most prominent influence on the ultimate strength of the column before 20 min fire exposure, but after that, its influence is insignificant. The column strength and fire-resistance generally decrease with an increase in the preload ratio.

References

1. V. Gayathri, N. E. Shanmugam, Y. S. Choo, Concrete-filled tubular columns: Part 1-Cross-section analysis, *Int. J. of Struct. Stab. Dyn.* **4**(4) (2004) 459-478.
2. V. Gayathri, N. E. Shanmugam, Y. S. Choo, Concrete-filled tubular columns: Part 2-Column analysis, *Int. J. of Struct. Stab. Dyn.* **4**(4) (2004) 479-495.
3. V. I. Patel, Q. Q. Liang, M. N. S. Hadi, High strength thin-walled rectangular concrete-filled steel tubular slender beam-columns, Part I: Modeling, *J. Constr. Steel Res.* **70** (2012) 377-384.
4. Q. Q. Liang, V. I. Patel, M. N. S. Hadi, Biaxially loaded high-strength concrete-filled steel tubular slender beam-columns, Part I: Multiscale simulation, *J. Constr. Steel Res.* **75** (2012) 64-71.
5. Eurocode 4, *Design of Composite Steel and Concrete Structures, Part 1.1: General Rules and Rules for Building*, British Standards Institution, London, UK (2014).
6. AISC 360-16, *Specification for Structural Steel Buildings*, American Institute of Steel Construction, Chicago, IL, USA (2016).
7. ACI-318-11, *Building Code Requirements for Reinforced Concrete*, American Concrete Institute, Detroit, MI (2011).

8. T. T. Lie, M. Chabot, Experimental studies on the fire resistance of hollow steel columns filled with plain concrete, *Internal report, National Research Council Canada, Institute for Research in Construction,* 1992-01 (1992).
9. Y. Sakumoto, T. Okada, M. Yoshida, S. Tasaka, Fire resistance of concrete-filled, fire resistant steel-tube columns. *J. Mat. in Civil Eng. ASCE* **69**(2) (1994) 169-184.
10. L. H. Han, Y. F. Yang, L. Xu, An experimental study and calculation on the fire resistance of concrete-filled SHS and RHS columns, *J. Constr. Steel Res.* **59** (2003) 427-452.
11. A. Espinos, M. L. Romero, E. Serra, A. Hospitaler, Circular and square slender concrete-filled tubular columns under large eccentricities and fire, *J. Constr. Steel Res.* **110** (2015) 90-100.
12. A. Espinos, M. L. Romero, E. Serra, A. Hospitaler, Experimental investigation on the fire behavior of rectangular and elliptical slender concrete-filled tubular columns, *Thin-Walled Struct.* **93** (2015) 137-148.
13. K. U. Ukanwa, J. B. P. Lim, U. K. Sharma, S. J. Hicks, A. Abu, G. C. Clifton, Behaviour and design of a continuous concrete filled steel tubular column in fire for a multi-storey building, *J. Constr. Steel Res.* **139** (2017) 280-287.
14. Y. F. Yang, L. Zhang, X. Dai, Performance of recycled aggregate concrete-filled square steel tubular columns exposed to fire, *Adv. in Struct. Eng.* **20**(9) (2017) 1340-1356.
15. Q. H. Tan, L. Gardner, L. H. Han, Performance of steel-reinforced concrete-filled stainless steel tubular columns at elevated temperature, *Int. J. of Struct. Stab. Dyn.* **19**(01) (2019) 1940002.
16. T. T. Lie, I. Dawod, Factors affecting the fire resistance of square hollow steel columns filled with plain concrete, *Internal Report (National Research Council Canada. Institute for Research in Construction)*, 1992-08 (1992).

17. T. T. Lie, R. J. Irwin, Fire resistance of rectangular steel columns filled with bar-reinforced concrete, *J. Struct. Eng. ASCE* **12**(5) (1995) 797-805.
18. L. H. Han, Fire performance of concrete filled steel tubular beam-columns, *J. Constr. Steel Res.* **57** (2001) 695-709.
19. K. Chung, S. Park, S. Choi, Fire resistance of concrete filled square steel tube columns subjected to eccentric axial load, *Steel Struct.* **9** (2009) 69-76.
20. J. Ding, Y. C. Wang, Realistic modelling of thermal and structural behaviour of unprotected concrete filled tubular columns in fire*, J. Constr. Steel Res.* **64** (2008)1086-1102.
21. S. D. Hong, A. H. Varma, Analytical modeling of the standard fire behavior of loaded CFT columns, *J. Constr. Steel Res*. **65** (2009) 54-69.
22. P. Schaumann, V. Kodur, O. Bahr, Fire behaviour of hollow structural section steel columns filled with high strength concrete, *J. Constr. Steel Res.* **65** (2009)1794-1802.
23. C. Ibanez, M. L. Romero, A. Hospitaler, Fiber beam model for fire response simulation of axially loaded concrete filled tubular columns, *Eng. Struct.* **56** (2013) 182-193.
24. M. Yu, X. X. Zha, J. Q. Ye, Y. Li, Fire responses and resistance of concrete-filled steel tubular frame structures, *Int. J. of Struct. Stab. Dyn.* **10**(2) (2010) 253-271.
25. Q. Q. Liang, Performance-based analysis of concrete-filled steel tubular beam-columns. Part I: Theory and algorithms*, J. Constr. Steel Res*. **65**(2) (2009) 363-373.
26. Q. Q. Liang, *Analysis and Design of Steel and Composite Structures,* 2014 (CRC Press, Boca Raton and London).
27. Q. Q. Liang, Nonlinear analysis of circular double-skin concrete-filled steel tubular columns under axial compression, *Eng. Struct.* 131 (2017) 639-650.
28. Eurocode 1, *Actions on Structures, Part 1.2: General Actions- Actions on Structures Exposed to Fire*, CEN, Brussels, Belgium, 2002.
29. Eurocode 3, *Design of Steel Structures, Part 1.2: General Rules-Structural Fire Design*, CEN, Brussels, Belgium, 2005.

30. Eurocode 2, *Design of Concrete Structures, Part 1.2: General Rules-Structural Fire Design*, CEN, 2004 (Brusssels, Belgium).

31. G. M. Kamil, Q. Q. Liang, M. N. S. Hadi, Numerical analysis of axially loaded rectangular concrete-filled steel tubular short columns at elevated temperatures, *Eng. Struct.* **180** (2019) 89-102.

32. H. Yang, L. H. Han, Y. C. Wang. Effects of heating and loading histories on post-fire cooling behaviour of concrete-filled steel tubular columns. *J. Constr. Steel Res.* **64**(5) (2008) 556-570.

33. G. M. Kamil, Q. Q. Liang, M. N. S. Hadi, Local buckling of steel plates in concrete–filled steel tubular columns at elevated temperatures, *Eng. Struct.* **168** (2018) 108-118.

34. Q. Q. Liang, B. Uy, J. Y. R. Liew, Local buckling of steel plates in concrete-filled thin-walled steel tubular beam-columns, *J. Constr. Steel Res.* **63**(3) (2007) 396-405.

35. Q. Q. Liang, High strength circular concrete-filled steel tubular slender beam-columns, Part I: Numerical analysis, *J. Constr. Steel Res.* **67**(2) (2011) 164-171.

36. V. I. Patel, Q. Q. Liang, M. N. S. Hadi, Numerical analysis of circular concrete-filled steel tubular slender beam-columns with preload effects, *Int. J. of Struct. Stab. Dyn.* **13** (3) (2013) 1250065.

37. D. E. Müller, A method for solving algebraic equations using an automatic computer, *MTAC* **10** (1956) 208-215.

38. K. Kordina, W. Klingsch, Fire resistance of composite columns of concrete filled hollow sections, *Research report. CIDECT 15 C1/C2-83/27*, (1983) Germany.

Figures and Tables

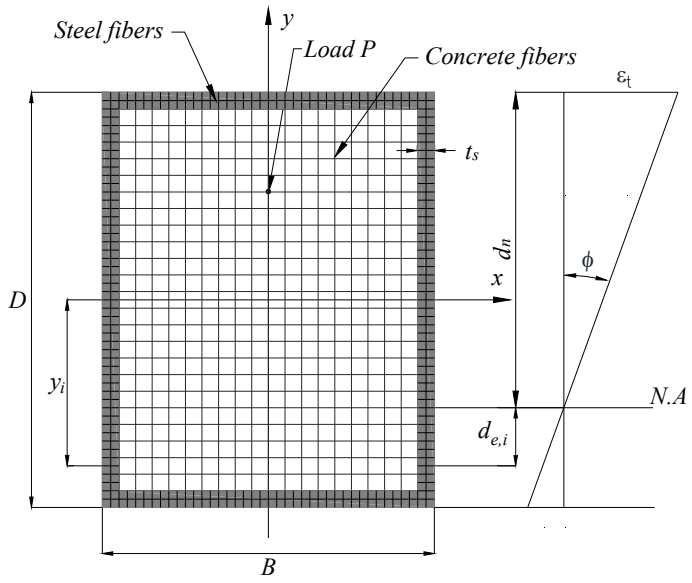

Fig. 1. Typical fiber mesh and strain distribution in the cross-section of a rectangular CFST column under uniaxial bending.

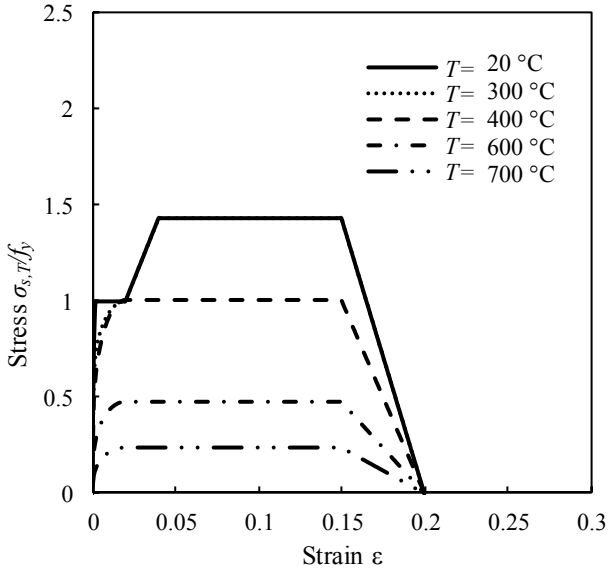

Fig. 2. Temperature-dependent stress-strain curves for structural steels in accordance with Eurocode 3.[29]

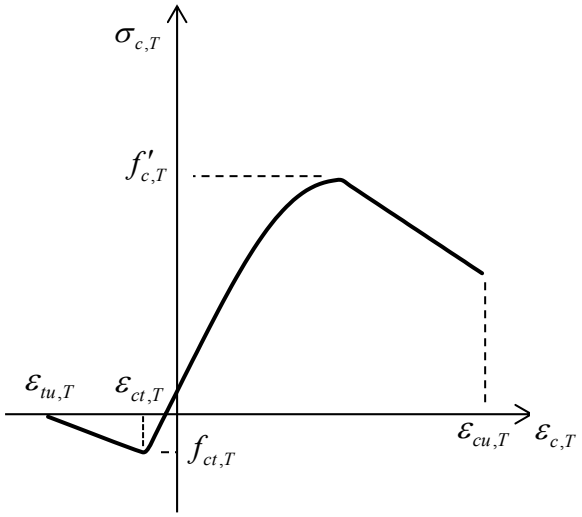

Fig. 3. Idealized temperature-dependent stress-strain curve for concrete.

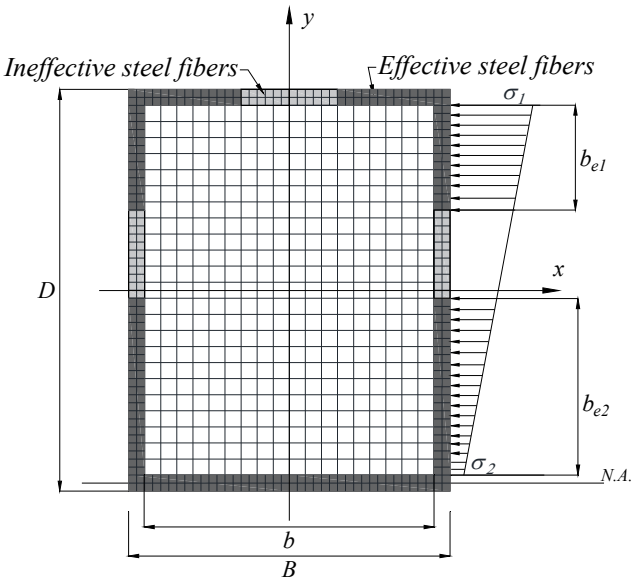

Fig. 4. Effective widths of steel tube walls in rectangular CFST column section under uniaxial bending.

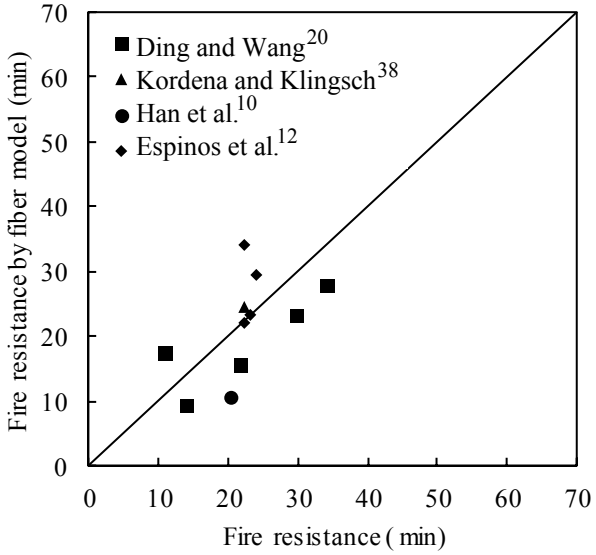

Fig. 5. Comparison of fire-resistance times predicted by the present fiber model with those obtained from testes and finite element analyses.

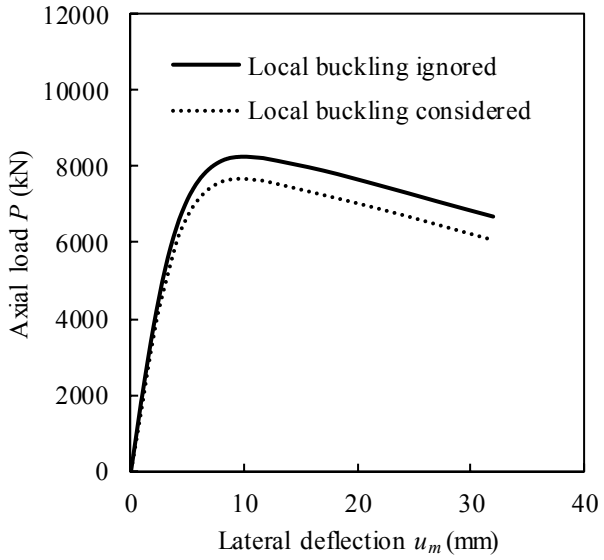

Fig. 6. Influences of local buckling on the axial load-deflection responses of slender square CFST column at the fire exposure time of 20 min.

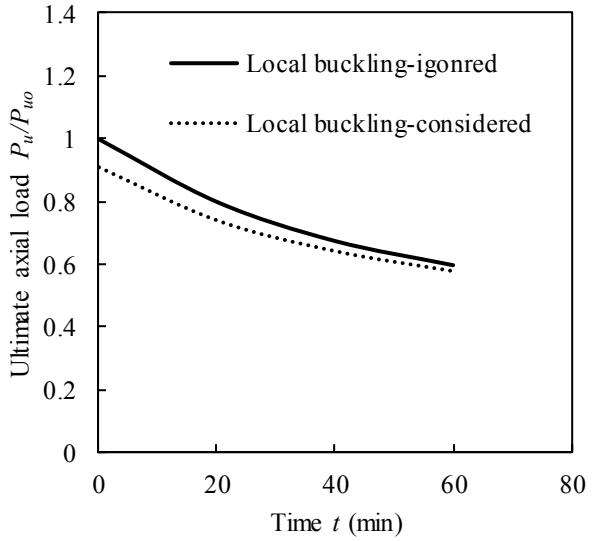

Fig. 7. Influences of local buckling on the column strength-fire exposure time curve.

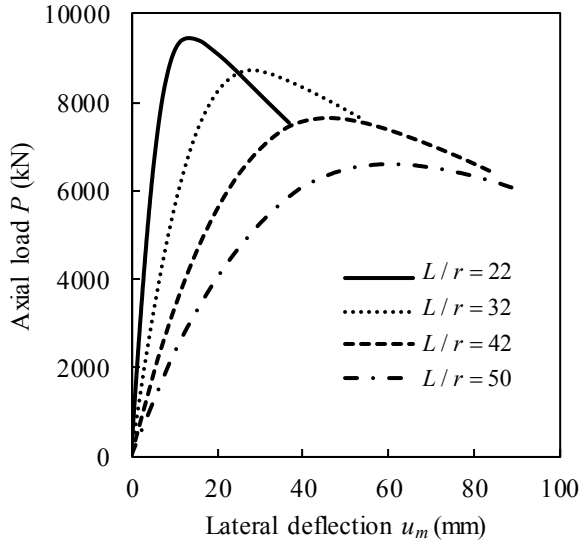

Fig. 8. Effects of column slenderness on the axial load-deflection responses of square CFST columns at the fire exposure time of 40 min.

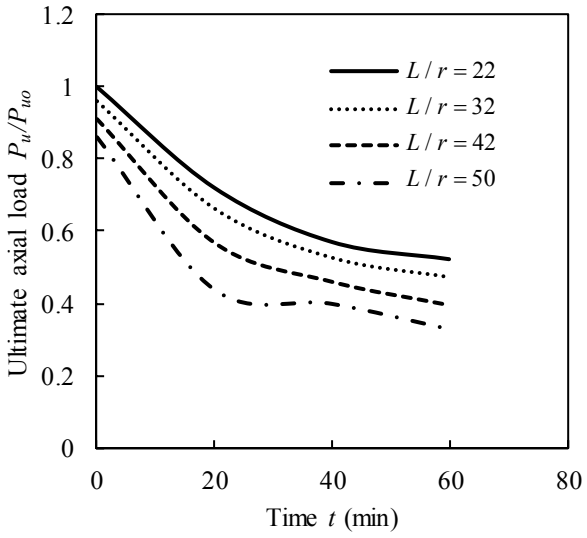

Fig. 9. Effects of column slenderness ratio on the column strength-fire exposure time curves.

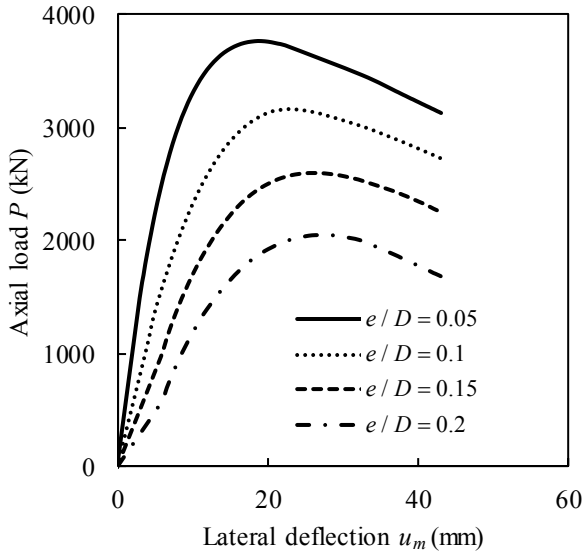

Fig. 10. Effects of e/D ratios on the structural responses of square slender CFST column at the fire exposure time of 40 min.

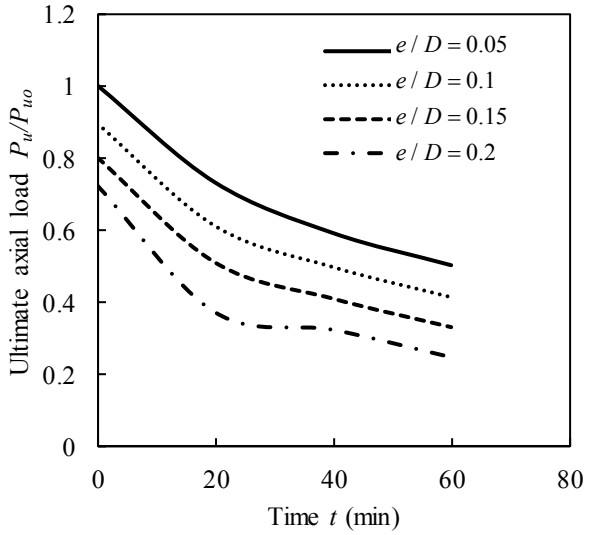

Fig. 11. Effects of e/D ratios on the column strength-fire exposure time curves.

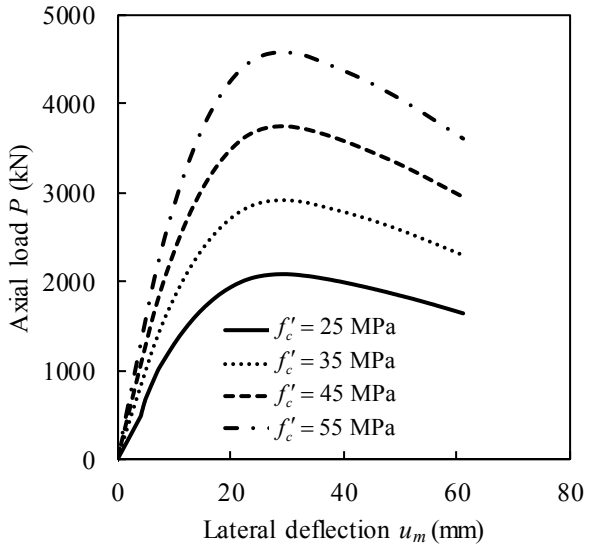

Fig. 12. Effects of concrete strength on the structural responses of rectangular slender CFST columns at the fire exposure time of 40 min.

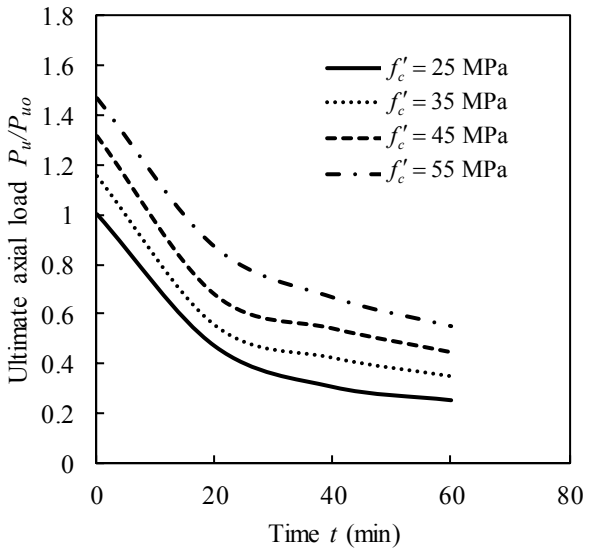

Fig. 13. Effects of concrete strengths on the column strength-fire exposure time curves.

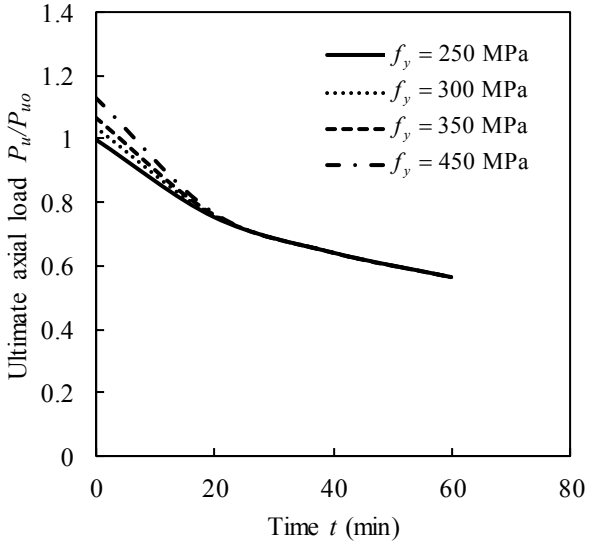

Fig. 14. Effects of the steel yield strength on the column strength-fire exposure time curves.

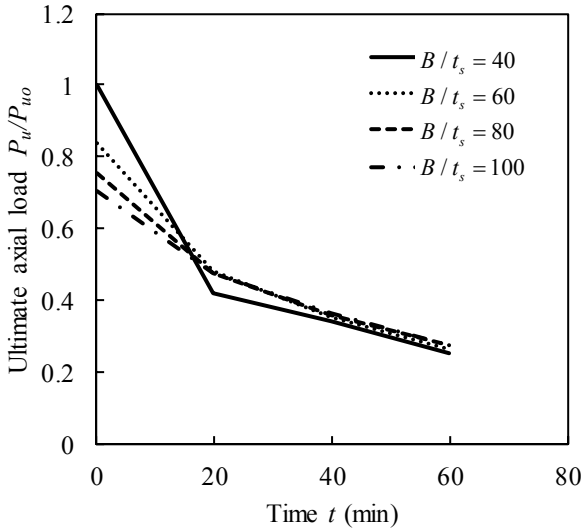

Fig. 15. Effects of B/t_s ratios on the column strength-fire exposure time curves.

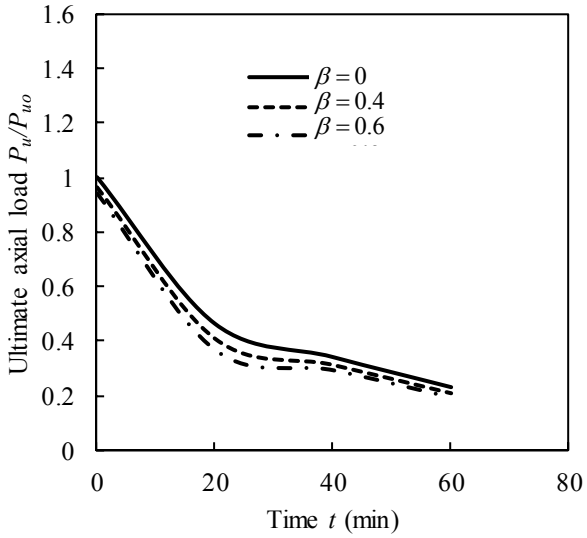

Fig. 16. Effects of preload ratios on the column strength-fire exposure time curves.

Table 1. Geometric and material properties of CFST slender columns

Specimen	($B\times D\times t_s$) (mm)	f_y (MPa)	f_c' (MPa)	L (mm)	P (kN)	e/D or e/B	Reference
R-4	150×300×7.96	341	40.5	3810	1853	0.075	Han *et al.*[10]
13	200×200×6.3	279	55	2940	400	0.1	Kordina and Klingsch[38]
R3	150×250×10	428.3	32	3180	374.7	0.2	Espinos *et al.*[12]
R5	150×250×10	457.7	36.5	3180	456.7	0.2	
R9	150×350×10	383.3	37.6	3180	540.1	0.2	
R11	150×350×10	383.3	38	3180	683	0.2	
B4b	200×200×12.5	275	30	3000	1185	0.1	Ding and Wang[20]
C4a	200×200×12.5	275	30	2100	1728	0.1	
C4b	200×200×12.5	275	30	3000	1728	0.1	
C2a	200×200×12.5	275	30	2100	740	0.1	
C2b	200×200×12.5	275	30	3000	740	0.1	